

## Direct Observation of C<sup>α</sup>–H<sup>α</sup>···O=C Hydrogen Bonds in Proteins by Interresidue <sup>h3</sup>J<sub>C<sup>α</sup>C' Scalar Couplings</sub>

Florence Cordier, Michael Barfield,\* and Stephan Grzesiek\*

Biozentrum, University of Basel, Basel 4056, Switzerland, and Department of Chemistry, University of Arizona, Tucson, Arizona 85721

Received September 19, 2003; E-mail: barfield@u.arizona.edu; stephan.grzesiek@unibas.ch

Albeit postulated early by Huggins<sup>1</sup> and Pauling,<sup>2</sup> C–H···O hydrogen bonds (H-bonds) have only slowly been recognized as rather common structural elements in chemistry<sup>3–6</sup> and biology.<sup>7,8</sup> In proteins, short C···O distances are usually observed for C<sup>α</sup>–H<sup>α</sup>···O=C configurations in β-sheets (Figure 1, right), but are more rare in helical structures.<sup>7,9,10</sup> Recent ultrahigh-resolution crystal structures of several proteins with resolved H<sup>α</sup> atoms give clear evidence for short (~2.4 Å) H<sup>α</sup>···O contacts in β-sheets<sup>11,12</sup> and also show that the H<sup>α</sup> positions deviate by about 0.2 to 0.3 Å from idealized C<sup>α</sup>–H<sup>α</sup> geometries, with the hydrogen being bent toward the oxygen acceptor.<sup>12</sup>

Little is known about the contribution of C–H···O H-bonds to the stability of biomacromolecules. Recent ab initio calculations<sup>13</sup> suggest association enthalpies ΔH<sup>298</sup> of –3 kcal mol<sup>–1</sup> for C<sup>α</sup>–H<sup>α</sup>···O=C H-bonds, which are roughly half the size of N–H···O=C energies calculated at the same level of theory. Here, we report the first NMR observation of H-bond scalar coupling (<sup>h3</sup>J<sub>C<sup>α</sup>C') correlations across C<sup>α</sup>–H<sup>α</sup>···O=C H-bonds in β-sheet regions of a small protein. Such correlations are direct evidence of the electronic wave function overlap of H-bond donor and acceptor groups. The size of the observed couplings (0.2 to 0.3 Hz) is in reasonable agreement with results of DFT calculations on corresponding protein fragments. Thus, the present study should provide reliable experimental limits for theoretical models of electronic wave functions and strengths of C<sup>α</sup>–H<sup>α</sup>···O=C H-bonds in proteins.</sub>

The observation of <sup>h3</sup>J<sub>C<sup>α</sup>C' correlations in proteins is considerably more difficult than for the conventional <sup>h3</sup>J<sub>N<sup>C'</sup></sub> couplings.<sup>14,15</sup> Significant losses in sensitivity arise from the fast relaxation of <sup>13</sup>C nuclei and from the presence of other homonuclear <sup>13</sup>C–<sup>13</sup>C scalar couplings, which are not easily refocused. An initial screen was performed with a long-range version of the constant-time H(NCO)CA pulse sequence<sup>16</sup> where the amide <sup>1</sup>H<sup>N</sup> frequencies of the amino acid following the carbonyl acceptor are correlated to the <sup>13</sup>C<sup>α</sup> frequency of the H-bond donor (Figure 1, right). In this experiment (Supporting Information), the <sup>13</sup>C' to <sup>13</sup>C<sup>α</sup> dephasing and rephasing times (2T<sub>C</sub>) had been set to a value of 113 ms ≈ 6/<sup>1</sup>J<sub>C<sup>α</sup>C'</sub> in order to refocus transfers from one-bond <sup>1</sup>J<sub>C<sup>α</sup>C'</sub> couplings and as a compromise between the fast decay of <sup>13</sup>C' magnetization and the efficient transfer by the small H-bond <sup>h3</sup>J<sub>C<sup>α</sup>C'</sub> couplings.</sub>

Figure 1 (left) shows results of this long-range H(NCO)CA carried out on the uniformly <sup>15</sup>N/<sup>13</sup>C/<sup>2</sup>H labeled (amide-protonated) immunoglobulin binding domain of protein G.<sup>17,18</sup> Among many other cross-peaks arising from not completely suppressed intrasidue <sup>1</sup>J<sub>C<sup>α</sup>C'</sub> and sequential <sup>2</sup>J<sub>C<sup>α</sup>C'</sub> correlations, four cross-peaks are visible, which are due to magnetization transfer by <sup>h3</sup>J<sub>C<sup>α</sup>C'</sub> couplings across C=O···H–C<sup>α</sup> H-bonds L10/E20, Y8/T22, F57/L10, and T60/G46. Similar to the quantitative long-range HNCO experiment,<sup>14</sup> the absolute size of the respective <sup>h3</sup>J<sub>C<sup>α</sup>C'</sub> couplings can be determined from a comparison of the cross-peak intensities in Figure 1 to intensities of the corresponding <sup>1</sup>J<sub>C<sup>α</sup>C'</sub> correlations in a second

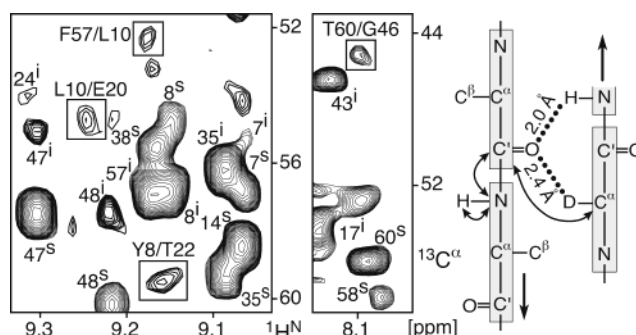


**Figure 1.** <sup>h3</sup>J<sub>C<sup>α</sup>C'</sub> magnetization transfer across protein C<sup>α</sup>–H<sup>α</sup>···O=C H-bonds observed by a long-range H(NCO)CA experiment. Right: Typical arrangement of C<sup>α</sup>–H<sup>α</sup>···O=C and N–H···O=C H-bonds in an antiparallel β-sheet. H(NCO)CA magnetization pathways are indicated by double arrows. Left: Small regions of the long-range H(NCO)CA experiment carried out on a 3.5 mM sample of protein G (25 °C); total experimental time 141 h. Boxed peaks represent transfers by <sup>h3</sup>J<sub>C<sup>α</sup>C'</sub> couplings and are labeled by H-bond acceptor/donor residue. Intrasidue <sup>1</sup>J<sub>C<sup>α</sup>C'</sub> (superscript i) and sequential <sup>2</sup>J<sub>C<sup>α</sup>C'</sub> (superscript s) correlations are labeled by the residue number of the <sup>13</sup>C' nucleus.

**Table 1.** Observed and Calculated <sup>h3</sup>J<sub>C<sup>α</sup>C'</sub> Values<sup>a</sup> in Protein G

donor C <sup>α</sup> –H	L10	E20	T22	G46	W48	F57
acceptor O=C	F57	L10	Y8	T60	T58	T49
<sup>h3</sup> J <sub>C<sup>α</sup>C'</sub> H(NCO)CA	0.26	0.28	0.30	0.28		
<sup>h3</sup> J <sub>C<sup>α</sup>C'</sub> H(NCA)CO		0.33			0.22	0.19
<sup>h3</sup> J <sub>C<sup>α</sup>C'</sub> DFT	0.12	0.56	0.17	0.09	0.38	0.26
<sup>h3</sup> J <sub>C<sup>α</sup>C'</sub> regression	0.13	0.53	0.15	0.10	0.43	0.23

<sup>a</sup> All values are given in Hz. Errors estimated from the noise of the experiments are about ±0.03 Hz.

reference experiment optimized for <sup>1</sup>J<sub>C<sup>α</sup>C'</sub> transfer (Supporting Information). Values of |<sup>h3</sup>J<sub>C<sup>α</sup>C'</sub>| for all four observed correlations (Table 1) are close to 0.3 Hz and are thus of similar order as <sup>h3</sup>J<sub>C<sup>α</sup>C'</sub> couplings.<sup>14,15</sup>

Clearly, the sensitivity of the long-range H(NCO)CA experiment is compromised by the presence of <sup>2</sup>J<sub>C<sup>α</sup>C'</sub> and <sup>3</sup>J<sub>C<sup>α</sup>C'</sub> couplings, which are not refocused during the extended transfer delays. These couplings can reach sizes of 2 to 3 Hz<sup>19</sup> and contribute attenuation factors of cos<sup>2</sup>(2πJ·T<sub>C</sub>) each. A certain improvement in sensitivity for detecting <sup>h3</sup>J<sub>C<sup>α</sup>C'</sub> can be obtained by selective transfer schemes and by making use of the favorable relaxation properties of <sup>13</sup>C<sup>α</sup> nuclei in deuterated proteins.<sup>20</sup> For this purpose, a selective, long-range H(NCA)CO pulse sequence was designed (see Supporting Information). In contrast to the common version of the experiment,<sup>21</sup> <sup>13</sup>C<sup>α</sup> to <sup>13</sup>C' dephasing and rephasing times were set to 6/<sup>1</sup>J<sub>C<sup>α</sup>C'</sub> to refocus unwanted <sup>1</sup>J<sub>C<sup>α</sup>C'</sub> transfers, and <sup>13</sup>C<sup>α</sup> 180° refocusing pulses were applied as highly selective sinc-pulses to minimize losses by <sup>3</sup>J<sub>C<sup>α</sup>C'</sub> couplings.

Figure 2 shows results of this long-range H(NCA)CO experiment applied selectively to the <sup>13</sup>C<sup>α</sup> resonances of residues E20, W48,

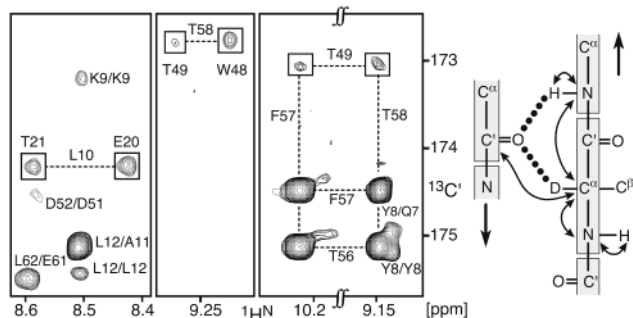


**Figure 2.**  $^{13}\text{C}_{\alpha\text{C}}$  magnetization transfer across protein  $\text{C}^{\alpha}\text{--H}^{\alpha}\cdots\text{O}=\text{C}$  H-bonds observed by selective long-range H(NCA)CO experiments. Right: Magnetization pathways of the H(NCA)CO. Left: Small regions of the long-range H(NCA)CO experiment carried out separately with selective excitation of the  $^{13}\text{C}_{\alpha}$  resonances of residues E20, W48, and F57 (from left to right). Boxed peaks represent transfers by  $^{13}\text{C}_{\alpha\text{C}}$  couplings. Peaks are labeled by the residue number of the  $^1\text{H}^{\text{N}}$  proton and of the  $^{13}\text{C}^{\alpha}$  nucleus. Total experimental times: 32 h (E20), 136 h (W48), and 145 h (F57).

and F57, respectively. In comparison to the nonselective H(NCO)CA, the sensitivity is considerably improved (e.g., H-bond E20– $\text{H}^{\alpha}\cdots\text{O}$ –L10). The identification of the H-bond connectivities is also more straightforward due to the reduced overlap and the presence of both  $\text{H}_{i+1}^{\text{N}}$  and  $\text{H}_i^{\text{N}}$  to  $\text{C}_i^{\alpha}$  magnetization transfers that are typical for HNCA-like experiments. Quantification of the  $^{13}\text{C}_{\alpha\text{C}}$  couplings is obtained in an analogous way as for the H(NCO)CA experiment (Supporting Information), and the values are listed in Table 1.

To compare the experimental  $^{13}\text{C}_{\alpha\text{C}}$  values to quantum chemical predictions, density functional theory (DFT) and finite perturbation theory (FPT) were used to obtain the Fermi contact (FC) contributions for these coupling constants (Table 1). The calculations were based on the coordinates of the IIGD crystallographic structure for protein G,<sup>18</sup> and the computational strategy (Supporting Information) was similar to that developed previously for  $^{13}\text{J}_{\text{NC}^{\alpha}}$  couplings.<sup>22</sup>

The average agreement between the experimental and predicted  $^{13}\text{C}_{\alpha\text{C}}$  is very reasonable. The remaining individual disparities can probably be attributed to large variations in the local molecular geometry around the H-bonds as well as to the recently demonstrated influence of dynamical averaging on H-bond couplings in proteins.<sup>23</sup> The relationship between scalar coupling in the  $\text{N--H}\cdots\text{O}=\text{C}$  moiety and the overlap integrals between the donor hydrogen and the oxygen hybrid orbitals leads to a  $\cos^2 \theta_2$  dependence<sup>22</sup> on the angle  $\theta_2$  ( $\angle\text{H}\cdots\text{O}=\text{C}$ ) and an exponential dependence<sup>22,24</sup> on the  $\text{H}\cdots\text{O}$  distance. Since the structural dependence of  $^{13}\text{C}_{\alpha\text{C}}$  in the  $\text{C}^{\alpha}\text{--H}^{\alpha}\cdots\text{O}=\text{C}$  moiety should be completely analogous, the DFT data were fit empirically to a form combining these features, i.e.,  $^{13}\text{C}_{\alpha\text{C}} = (4.6 \times 10^3 \text{ Hz})(\cos^2 \theta_2) \exp(-4.0 \text{ \AA}^{-1} \cdot r_{\text{H}\alpha\text{O}})$ , where  $\theta_2$  is the  $\text{H}^{\alpha}\cdots\text{O}=\text{C}$  angle and  $r_{\text{H}\alpha\text{O}}$  is the  $\text{H}^{\alpha}\cdots\text{O}$  distance. The standard deviation for the fit is 0.03 Hz, and the correlation coefficient  $r^2 = 0.97$ . The regression results are entered in the last row of Table 1.

The observed  $^{13}\text{C}_{\alpha\text{C}}$  correlations correspond to six out of 12  $\text{C}^{\alpha}\text{--H}^{\alpha}\cdots\text{O}=\text{C}$  H-bonds with  $\text{H}^{\alpha}\cdots\text{O}$  distances of less than 2.5 Å in protein G (Figure 3A). Because of the geometry of the bifurcated  $\text{H}^{\text{N}}\cdots\text{O}\cdots\text{H}^{\alpha}$  H-bonds in  $\beta$ -sheets (Figures 1 and 2), an anticorrelation

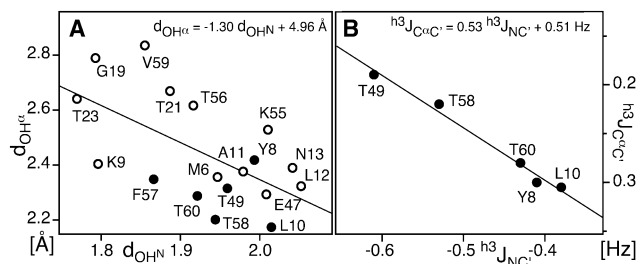


**Figure 3.** Anticorrelation of strengths of  $\text{C}^{\alpha}\text{--H}^{\alpha}\cdots\text{O}=\text{C}$  and  $\text{N--H}^{\text{N}}\cdots\text{O}=\text{C}$  H-bonds sharing the same carbonyl acceptor in protein G. (A)  $\text{H}^{\alpha}\cdots\text{O}/\text{H}^{\text{N}}\cdots\text{O}$  distance anticorrelation. Observed  $\text{C}^{\alpha}\text{--H}^{\alpha}\cdots\text{O}=\text{C}$  correlations are indicated by filled circles. (B)  $^{13}\text{C}_{\alpha\text{C}}/^{13}\text{J}_{\text{NC}^{\alpha}}$  anticorrelation. Data are labeled by the acceptor residue. Solid lines present linear regressions.

exists between the respective  $\text{H}^{\alpha}\cdots\text{O}$  and  $\text{H}^{\text{N}}\cdots\text{O}$  distances (Figure 3A).<sup>8</sup> This anticorrelation is also clearly visible (Figure 3B) when comparing the  $^{13}\text{C}_{\alpha\text{C}}$  values to the respective previously published  $^{13}\text{J}_{\text{NC}^{\alpha}}$  values.<sup>24</sup> Thus, both types of coupling constants appear as reliable reporters of wave function overlap and geometry in protein H-bonds.

**Acknowledgment.** This work was supported by SNF grant 31-61'757.00.

**Supporting Information Available:** Pulse schemes and experimental details of the long-range H(NCO)CA and H(NCA)CO experiments and details of the DFT calculations of  $^{13}\text{C}_{\alpha\text{C}}$  couplings (PDF). This material is available free of charge via the Internet at <http://pubs.acs.org>.

## References

- Huggins, M. L. *Chem. Rev.* **1943**, *32*, 195–218.
- Pauling, L. *The Nature of the Chemical Bond*; Cornell University Press: Ithaca, NY, 1960.
- Sutor, D. J. *Nature* **1962**, *195*, 68–69.
- Taylor, R.; Kennard, O. *J. Am. Chem. Soc.* **1982**, *104*, 5063–5070.
- Desiraju, G. R. *Acc. Chem. Res.* **1991**, *24*, 290–296.
- Steiner, T. *Chem. Commun.* **1997**, 727–734.
- Derewenda, Z. S.; Lee, L.; Derewenda, U. *J. Mol. Biol.* **1995**, *252*, 248–62.
- Wahl, M. C.; Sundaralingam, M. *Trends Biochem. Sci.* **1997**, *22*, 97–102.
- Bella, J.; Berman, H. M. *J. Mol. Biol.* **1996**, *264*, 734–42.
- Madan Babu, M.; Kumar Singh, S.; Balaran, P. *J. Mol. Biol.* **2002**, *322*, 871–80.
- Esposito, L.; Vitagliano, L.; Sica, F.; Sorrentino, G.; Zagari, A.; Mazzarella, L. *J. Mol. Biol.* **2000**, *297*, 713–732.
- Addlagatta, A.; Krzywda, S.; Czapinska, H.; Otlewski, J.; Jaskolski, M. *Acta Crystallogr., Sect. D* **2001**, *57*, 649–663.
- Vargas, R.; Garza, J.; Dixon, D. A.; Hay, B. P. *J. Am. Chem. Soc.* **2000**, *122*, 4750–4755.
- Cordier, F.; Grzesiek, S. *J. Am. Chem. Soc.* **1999**, *121*, 1601–1602.
- Cornilescu, G.; Hu, J.-S.; Bax, A. *J. Am. Chem. Soc.* **1999**, *121*, 2949–2950.
- Grzesiek, S.; Bax, A. *J. Magn. Reson.* **1992**, *96*, 432–440.
- Gronenborn, A. M.; Filpula, D. R.; Essig, N. Z.; Achari, A.; Whitlow, M.; Wingfield, P. T.; Clore, G. M. *Science* **1991**, *253*, 657–61.
- Derrick, J. P.; Wigley, D. B. *J. Mol. Biol.* **1994**, *243*, 906–18.
- Hu, J. S.; Bax, A. *J. Am. Chem. Soc.* **1996**, *118*, 8170–8171.
- Grzesiek, S.; Anglister, J.; Ren, H.; Bax, A. *J. Am. Chem. Soc.* **1993**, *115*, 4369–4370.
- Clubb, R. T.; Thanabal, V.; Wagner, G. *J. Magn. Reson.* **1992**, *97*, 213–217.
- Barfield, M. *J. Am. Chem. Soc.* **2002**, *124*, 4158–4168.
- Markwick, P. R. L.; Sprangers, R.; Sattler, M. *J. Am. Chem. Soc.* **2003**, *125*, 644–645.
- Cornilescu, G.; Ramirez, B. E.; Frank, M. K.; Clore, G. M.; Gronenborn, A. M.; Bax, A. *J. Am. Chem. Soc.* **1999**, *121*, 6275–6279.

JA038616M